International Journal of Embedded and Wireless Communication Systems
Volume1, Issue 2 2025

An Efficient Image Enlargement Method for Image Sensors of Mobile in Embedded Systems

Manita Rajput
Fr.C.Rodrigues Institute of Technology,Vashi, Mumbai Maharshtra,INDIA

Research Article

Date of Submission: 11-02-2025 **Date of Acceptance: 10-04-2025** **Date of Publication: 22-05-2025**

Abstract

Main challenges for image enlargement methods in embedded systems come from the requirements of good performance, low computational cost, and low memory usage. This paper proposes an efficient image enlargement method which can meet these requirements in embedded system. Firstly, to improve the performance of enlargement methods, this method extracts different kind of features for different morphologies with different approaches. Then, various dictionaries based on different kind of features are learned, which represent the image in a more efficient manner. Secondly, to accelerate the enlargement speed and reduce the memory usage, this method divides the atoms of each dictionary into several clusters. For each cluster, separate projection matrix is calculated. This method reformulates the problem as a least squares regression. The high-resolution (HR) images can be reconstructed based on a few projection matrixes. Numerous experiment results show that this method has advantages such as being efficient and real-time and having less memory cost. These advantages make this method easy to implement in mobile embedded system.

1. Introduction

Mobile phones have been a common part of people's lives during the last several decades. In 2017, there will be almost 5.3 billion mobile phone users worldwide. Many people use their phones not only for verbal communication but also as a means of taking pictures. The ability to take pictures and film videos anywhere at any time is one of the many advantages that mobile phones provide to its users. Unfortunately, due to the poor quality of the image sensor, many photos shot with mobile phones have low resolution. There are two ways to get high-resolution photos: (1) swap out the phone with a more powerful one; or (2) expand the photos using certain techniques. Instead of switching to a more powerful phone, the majority of mobile phone users would rather utilize a technique to expand the picture. Over the last ten years, a lot of work has been done on picture magnification techniques. However, when used in embedded systems, the expansion approaches encounter three difficulties: (1) performance requirements, (2) real-time requirements, and (3) memory consumption constraints.Superresolution (SR) is one of the most prospective image enlargement methods. Existing SR methods can be divided into three categories: interpolation-based methods [1, 2], reconstruction-based methods [3–5], and example-
based methods [6–10].

The interpolation-based methods [1, 2] apply the correla-tion of neighboring image pixels to approximate the funda-mental HR pixels. These types of methods have lower com-putation complexities. However, the interpolation does not add any new detailed information into the enlarged image. The quality of the enlarged image is still unsatisfying and it may cause the aliasing to the enlarged LR image. Although the interpolation-based methods run fast and need little memory, the poor performance limits the application of interpolation-based methods for the implementation in embedded system. Reconstruction-based methods [3–7] require different
LR images of the same scene taken from slightly moved viewpoints, and those LR images have different subpixel shifts from each other. This category of methods tries to exploit additional information from a sequence of successive LR images of the same scene to synthesize HR images. Compared with interpolation-based methods, the reconstruction-based methods obtain better performance with a small desired magnification factor. However, the performance of this kind of methods degrades rapidly when the desired magnification factor becomes large. The reconstruction-based methods need to store the information of all the sequence LR images, which is high memory requirement. Due to the above reasons, reconstruction-based methods are not ready for embedded system.

Single image SR methods such as neighbor embedding-based methods [7, 8], regression-based methods [9, 10], and sparse representation-based methods [11–15] have been explored in recent years. These methods presume that the high-frequency details lost in the LR images can be predicted through learning the cooccurrence relationship between LR training patches and their corresponding HR patches. Recently, sparse representation-based methods have proven to be effective towards solving image superresolution prob-lems. Yang et al. [16] proposed an approach based on sparse representation, with

the assumption that the HR and LR images share the same set of sparse coefficients. Therefore, the HR image can be reconstructed by combining the trained HR dictionary and the sparse coefficients of the corresponding LR image. Although the sparse representation-based meth-ods offer a good performance, the optimization of dictionary learning and image reconstruction has a problem of highly intensive computation. Besides, sparse representation-based SR methods reserve memory to store the information of HR dictionary and LR dictionary. The size of dictionary impacts the memory usage. Sparse representation-based SR methods require intensive large memory, especially with increasing size of dictionary. Both the time-complexity and memory usage are key limit factors in the embedded system applica-tions of these methods. Zhan et al. [17] proposed a fast mul-ticlass dictionaries learning method in MRI reconstruction. Timofte et al. [18] constructed a set of mapping relationships between the LR and HR patches using a learned LR-HR dictionary. Anchored Neighborhood Regression method [18] reformulates the problem as a least squares regression, which leads to a vast computational speedup while keeping the same accuracy as previous methods. Anchored Neighborhood Regression method calculates the mapping matrix based on a universal dictionary. However, a large number of different structural patterns exist in an image, whereas one dictionary is not capable of capturing all of the different morphologies. Besides, Anchored Neighborhood Regression method still needs to store separate projection matrix for each dictionarykey limit factors in the embedded system applications of these methods. The optimization of dictionary learning and image reconstruction leads to highly intensive computation. Sparse representation-based methods need to reserve memory to store the information of HR dictionary and LR dictionary. The size of dictionary impacts the memory usage.

Above all, this study makes the following three main contributions. (1) Jointly representing an image with different types of features is proposed in feature extraction stage. For accurately representing different morphologies, images (or patches) prefer different types of features extracted by differ-ent approaches, since one single feature extraction approach cannot accurately capture the essential features of the image.
(2) Multiple dictionaries are learned based on different types of features in sparse representation stage, since one dictionary with single type of features is inadequate in capturing all of the different morphologies of the image. To capture the differ-ent morphologies of the image more accurately, multifeature dictionaries, which consist of different dictionaries with dif-ferent features, are learned. (3) To reduce the computational cost and memory usage, we propose an Anchored Cluster Regression method. Anchored Cluster Regression method divides the dictionary atoms into several clusters. Then, the projection matrix for each cluster is calculated. In Anchored Cluster Regression method, each HR patch can be recon-structed by the projection matrix of its corresponding cluster. Anchored Cluster Regression method reformulates the prob-lem as a least squares regression. It only needs to store the pro-jection matrix of each cluster. Anchored Cluster Regression leads to a vast computational speedup and needs less memory.

2. Sparse Representation-Based SR Method

Superresolution aims to reconstruct the HR image from the LR image, which can be formulated as follows:

$$Y = HBX, \quad (1)$$

where ^{N} is the observed low-resolution (LR) image. $Y \in R$ ^{NL} is its corresponding high-resolution (HR) image $X \in R$ of the same scene. Y is a downsampled and blurred version

Similarly, the corresponding HR patch Patch x is with always suffer from three main problems for embedded sys-tem. First, the performance of these methods is limited, since these methods only use one approach to extract the features of the image for presenting the LR image generally. However, the morphologies vary significantly across images. Different patches prefer different features for accurately representing different morphologies. A single feature extraction approach cannot represent the image accurately. Therefore, jointly representing an image with different kind of features is impor-tant. Furthermore, time-complexity and memory usage are the size $\sqrt{nL} \times \sqrt{nL}$ at the location i, $i = 1, 2, \ldots, C$. And we have

3. The Proposed SR Method

The proposed method can be divided into three steps:
(a) learning different dictionary based on different mor-phologies, (b) calculating the projection matrixes, and (c) reconstructing the HR mobile sensor image.

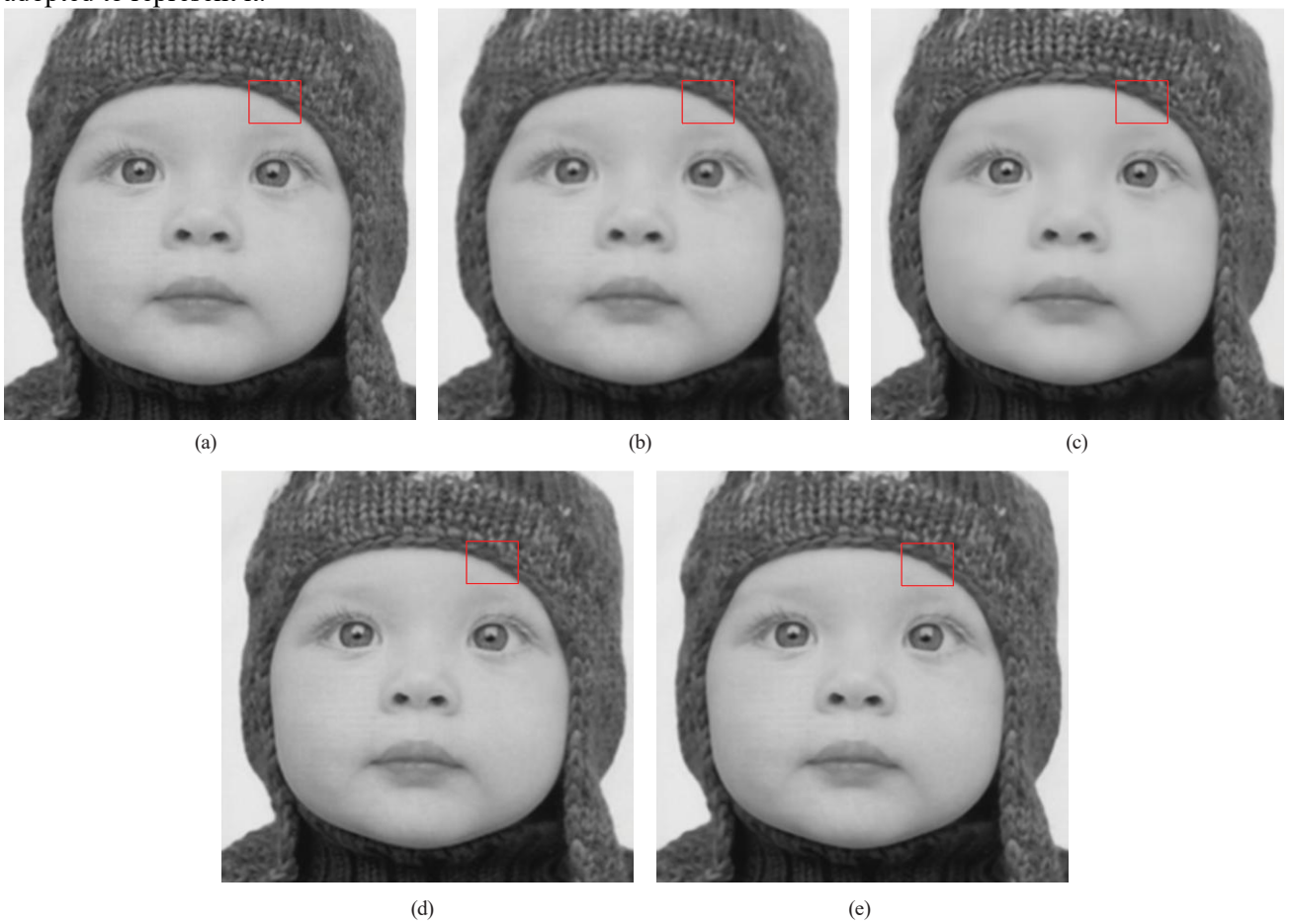
3.1. Learning the Dictionaries Based on Different Features. Most existing sparse representation-based SR methods use only derivative features to represent the morphologies of LR image. However, the artifacts would occur when using

which characterizes the LR patches. This projection produces a sparse representation of ^{i} via ^{i}:

$$y^{i} = D_l \alpha^{i} \qquad y^{i} \in R^{n}, \alpha^{i} \ll k, \qquad (6)$$

inappropriate features. An explanation for this phenomenon is that dictionary learning from only one kind of features cannot represent essential morphologies of the images. Since

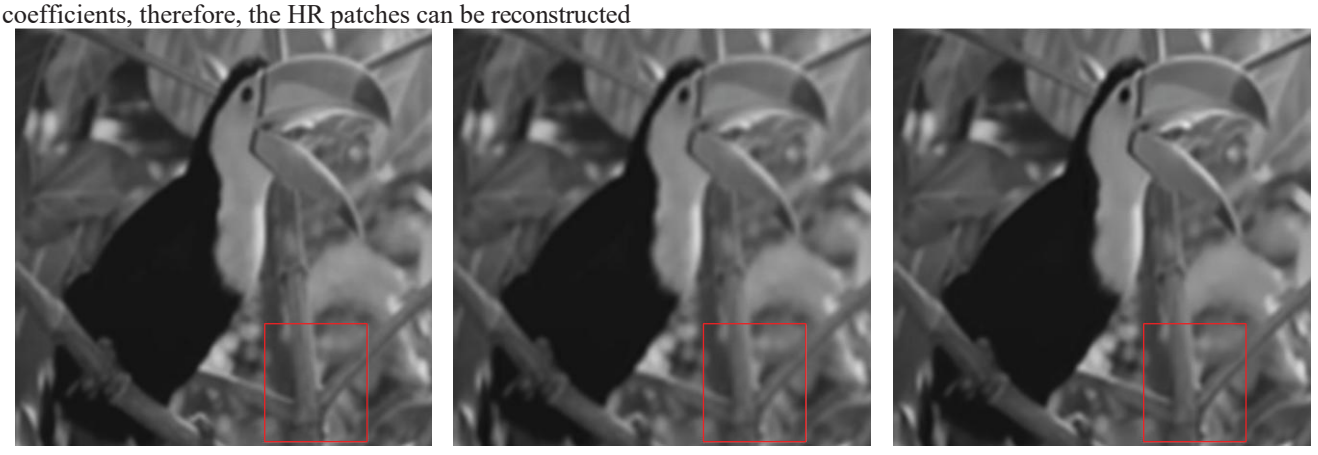
be adopted to represent it:



(a) (b) (c) (d) (e)

FIGURE 3: Visual comparison of baby: (a) original HR image, (b) results obtained using Cubic B-spline method, (c) results obtained using Yang's method, (d) results obtained using the ANR method, and (e) results obtained using our method.

Since sparse representation-based SR methods assume that the HR and LR images share the same set of sparse coefficients, therefore, the HR patches can be reconstructed



(a) (b) (c)

FIGURE 4: Visual comparison of bird: (a) original HR image, (b) results obtained using Cubic B-spline method, (c) results obtained using Yang's method, (d) results obtained using the ANR method, and (e) results obtained using our method.

leads to a vast computational speedup. However, Anchored Neighborhood Regression method still needs to store separate projection matrix for each dictionary atom which is high memory usage. Memory usage is key limit factor in the embedded system application for Anchored Neighborhood Regression methods.

To reduce the memory usage, we propose an Anchored Cluster Regression method. This method divides the atoms

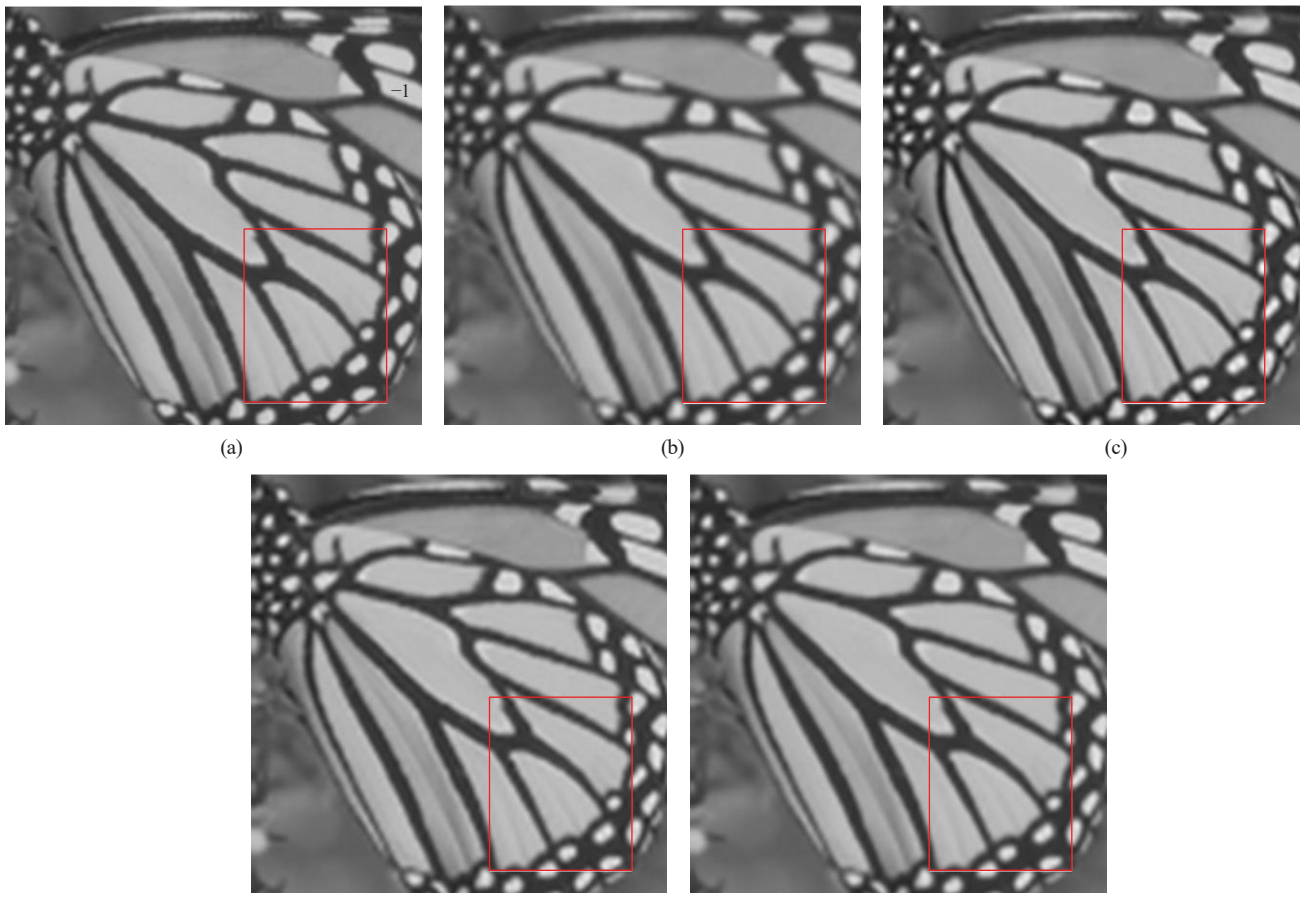
tering. Then, separate projection matrix P^k of each cluster is calculated. Then, use the projection matrix of the nearest cluster to reconstruct the HR patch:

$$x^{i,k} = P^k y^i_t \tag{19}$$

Anchored Cluster Regression method only needs to store the projection matrix of each cluster rather than the projection matrix of each atom. If atoms are divided into clusters, Anchored Cluster Regression method only needs

Neighborhood Regression needs to store projection matrix of each atom. Anchored Cluster Regression significantly reduces the memory. Furthermore, the computational complexity of Anchored Cluster Regression method is while complexity of Anchored Neighborhood Regression is of clusters. Anchored Cluster Regression significantly reduces the computation.

where N_c is the number of atoms and K is the number



(a) (b) (c)

(d) (e)

FIGURE 5: Visual comparison of butterfly: (a) original HR image, (b) results obtained using Cubic B-spline method, (c) results obtained using Yang's method, (d) results obtained using the ANR method, and (e) results obtained using our method.

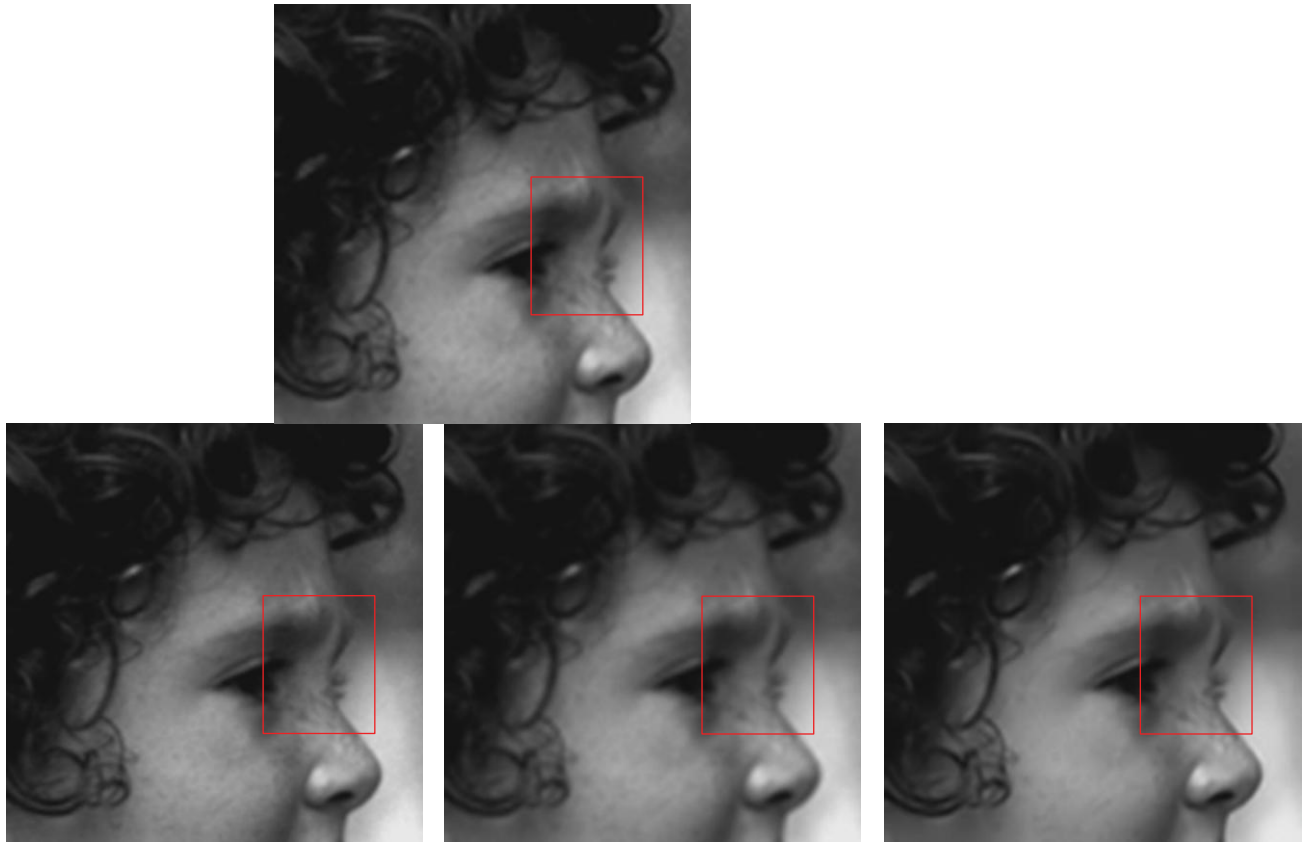
gether to get a final reconstructed HR image $\hat{x}^i$ of HR patch$_{k=1}$

into multiple clusters. The projection matrix of each cluster is calculated by (19)–(21).

In the reconstruction phase, for each LR patch, features of different morphologies are first extracted. Then, for each type of features, the nearest clusters in its corresponding morphology dictionaries are found. Based on the projection matrixes of these clusters, multiple estimated HR patches are reconstructed in the final stage. Then, the final HR patches are generated by using weighting average to process all estimated HR patches. Ultimately, the HR image is composed through averaging the overlapping reconstructed patches. The algorithm is illustrated in Figure 1.

4. Experimental Results

In our experiments, we use the same training set as [18],



(a) (b) (c)

FIGURE 6: Visual comparison of head: (a) original HR image, (b) results obtained using Cubic B-spline method, (c) results obtained using Yang's method, (d) results obtained using the ANR method, and (e) results obtained using our method.

[18]. The Set 5 datasets contain 5 images. The test images are shown in Figure 2. The low-resolution images used in all experiments are downsampled from the high-resolution images. In our experiments, low-resolution images are gener-ated by shrinking the corresponding high-resolution images with the scale factor of 3.

abor filters [21] have similar frequency and orientation representations to those of the human visual system. In the spatial domain, a 2D Gabor filter can be generated by Gaussian kernel function modulated with a sinusoidal plane wave. We employed Gabor features to represent the texture structure, since Gabor features can effectively characterize the texture representation and discrimination of LR patch. Gabor features of the image are extracted by convolving the normalized images with a family of Gabor filter (in this study, we use 2 scales and 4 orientations). Beside, we use derivative features representing high-frequency morphology structure of the image.means that the features are Gabor features.

means that the features are derivative features.

X

In the low-resolution images, we always use 3 3 low-resolution patches, with overlap of 1 pixel between adjacent patches, corresponding to 9 9 patches with overlap of 3 pixels for the high-resolution patches. 10000 pairs of low- and high-resolution patches are randomly chosen from the patch pairs generated by training images for dictionaries training.

Not only visual comparison but also quantitative com-parisons are confirming the superiority of the proposed method. Peak signal-to-noise ratio (PSNR) and the structural similarity measurement (SSIM) have been implemented in order to obtain some quantitative results for comparison. The values of the PSNR and SSIM of all of the test images were used as the quality index. The PSNR evaluates the reconstruction quality based on the pixel intensity. The SSIM measures the similarity between two images based on their structural information. The SSIM metric needs a "perfect" reference image for comparison and provides a normalized value within , where "0" indicates that the two images are totally different, whereas "1" confirms that the two images are the same. Thus, higher values of PSNR and SSIM indicate a result with better quality.

4.1. The Effect of Dictionaries with Multifeatures. To validate the effect of dictionaries with multiple features, we compared our method with the derivative feature-based method and Gabor feature-based method. In our method, we use Gabor features to characterize the texture of the image and derivative

FIGURE 7: Visual comparison of woman: (a) original HR image, (b) results obtained using Cubic B-spline method, (c) results obtained using Yang's method, (d) results obtained using the ANR method, and (e) results obtained using our method.

features represent high-frequency morphology structure of the image. These two features are used together to present the image. The derivative feature-based method adopted deriva-tive features to represent the LR image. And dictionaries with the derivative features were used to sparsely represent the LR patch. Similarly, Gabor feature-based method adopted Gabor features to represent the LR image. And dictionaries with the Gabor features were used to sparsely represent the LR patch. The PSNR and SSIM values of the SR results using various methods are listed in Table 1. We can observe that the proposed framework has a better performance than the single feature-based methods in terms of both PSNR and SSIM. This is due to the reason that one single feature extraction approach cannot accurately capture all the essential features of the image. Multitype features can jointly represent different morphologies in the image more accurately, so that different dictionaries with multitype features can represent the image in a more efficient manner and provide a more global look of the image, which would lead to the fact that the proposed

TABLE 1: Effects of multifeatures.

Method	Gabor features PSNR/SSIM	Derivative features PSNR/SSIM	Multiple features PSNR/SSIM
Baby	33.67/0.681	34.69/0.731	**35.09/0.743**
Bird	32.43/0.761	33.16/0.783	**34.42/0.802**
Butterfly	24.65/0.658	24.58/0.647	**25.79/0.680**
Head	29.46/0.673	33.19/0.712	**33.56/0.728**
Woman	24.94/0.578	29.86/0.683	**30.16/0.693**

complexity of Anchored Neighborhood Regression is $O(N)$. Anchored Cluster Regression method only needs to store the projection matrix of each cluster rather than the projection matrix of each atom. The size of projection matrix is.

If N atoms are divided into K clusters, Anchored Cluster Regression method only needs to store K projection matrix of each cluster. The computational complexity of Anchored Cluster Regression method is $O(K)$.

TABLE 2: Numerical results of Figures 3–7.

	Cubic B-spline PSNR/SSIM/time (second)	Yang's PSNR/SSIM/time (second)	ANR PSNR/SSIM/time (second)	Our method PSNR/SSIM/time (second)
Baby	33.91/0.697/0	34.29/0.726/56.06	34.90/0.738/0.98	**35.09/0.743/0.8**
Bird	32.58/0.768/0	34.11/0.789/22.33	34.38/0.794/0.29	**34.42/0.802/0.24**
Butterfly	24.04/0.632/0	25.58/0.674/20.22	25.82/0.687/0.24	**25.79/0.680/0.20**
Head	32.88/0.704/0	33.17/0.709/15.58	33.44/0.716/0.28	**33.56/0.728/0.26**
Woman	28.56/0.679/0	29.94/0.687/19.04	**30.17**/0.693/0.27	30.16/**0.693/0.23**

We first presented the superresolution results by different methods in Figures 3–7. Then, the zoomed version of the marked

areas of Figures 3–7 is shown in Figure 8. We see that the Cubic B-spline interpolation methods blurred the edges and lost some dedicated details in the resultant images. Although Yang's method recovered plenty of details, it produced many jaggy and ringing artifacts along with the edges or details. The reason for this is that a single type of features is unable to completely represent various structures of the image. On the contrary, with the proposed framework, images were presented with sharp edges but fewer artifacts. Different dictionaries with multitype features were used to represent the LR image and the weights of different HR patches were also adaptively adjusted in the proposed framework. That is why the proposed framework obtained a better visual quality than all the other three methods.

Moreover, the PSNR and SSIM values of superresolution results using various algorithms are listed in Table 2. We can see the PSNR and SSIM gains of proposed framework over the other methods, which demonstrates that the superresolution results with the proposed framework have better objective quality than other methods in terms of PSNR and SSIM indexes. All this illustrates that the proposed framework is the best one among the compared methods in terms of visual perception and objective quality.

In addition, from Table 2, we see that the time consump-tion of Cubic B-spline interpolation methods is 0 seconds. That is because Cubic B-spline is an interpolation-based method which is the simplest and the fastest. We can find that Yang's method is consistently the most time-consuming, because it needs to solve a least squares optimization and an iterative convex optimization. Due to reformulating the SR problem as a least squares regression, our method runs a little faster than Anchored Neighborhood Regression method, that is, because it only needs to search the nearest cluster in our method rather than searching the nearest atom in Anchored Neighborhood Regression method. Besides, our method significantly reduces the memory usage, which is suitable for embedded system applications.

5. Conclusion

A novel SR enlargement technique for mobile sensor images is presented in this research. First, complex information in natural pictures is best captured by various morphological components and multimorphology dictionaries learnt from corresponding morphological training sets in order to more properly depict mobile sensor images. The atoms for every dictionary

are separated into many groups in order to compute the projection matrix. Next, adaptive control is applied to the weights of the HR patches derived from various projection matrices. Experiments have shown that the suggested framework is superior to other comparative methodologies in terms of both visual perception and quantitative comparisons. This approach is simple to use in mobile embedded system applications since matrix multiplication is the scheme's primary calculation and it uses little memory.

References

Computer Society Conference on Computer Vision and Pattern Recognition (CVPR '04), vol. 1, pp. 275–282, July 2004.

K. Zhang, X. Gao, X. Li, and D. Tao, "Partially supervised neigh-bor embedding for example-based image super-resolution," IEEE Journal on Selected Topics in Signal Processing, vol. 5, no. 2,
pp. 230–239, 2011.

X. Wang and X. Tang, "Hallucinating face by eigen transforma-tion," IEEE Transactions on Systems, Man, and Cybernetics, Part C, vol. 35, no. 3, pp. 425–434, 2005.

W. Wu, Z. Liu, and X. He, "Learning-based super resolution using kernel partial least squares," Image and Vision Computing, vol. 29, no. 6, pp. 394–406, 2011.

M. Aharon, M. Elad, and A. Bruckstein, "K-SVD: an algorithm for designing overcomplete dictionaries for sparse representa-tion," IEEE Transactions on Signal Processing, vol. 54, no. 11, pp. 4311–4322, 2006.

G. Monaci and P. Vandergheynst, "Learning structured dictio-naries for image representation," in Proceedings of the Interna-tional Conference on Image Processing (ICIP '04), pp. 2351–2354, IEEE, October 2004.

R. Zeyde, M. Elad, and M. Protter, "On single image scale-up using sparse-representations," in Curves and Surfaces, J.-D. Boissonnat, P. Chenin, A. Cohen et al., Eds., vol. 6920 of Lecture Notes in Computer Science, pp. 711–730, Springer, New York, NY, USA, 2012.

K. Zhang, X. Gao, D. Tao, and X. Li, "Single image super-resolution with non-local means and steering kernel regres-sion," IEEE Transactions on Image Processing, vol. 21, no. 11, pp. 4544–4556, 2012.

X. Yang, K. Liu, Z. Gan, and B. Yan, "Multiscale and multitopic sparse representation for multisensor infrared image superres-olution," Journal of Sensors, vol. 2016, Article ID 7036349, 14 pages, 2016.

J. Yang, J. Wright, T. S. Huang, and Y. Ma, "Image super-resolution via sparse representation," IEEE Transactions on Image Processing, vol. 19, no. 11, pp. 2861–2873, 2010.

Z. Zhan, J. Cai, D. Guo, Y. Liu, Z. Chen, and X. Qu, "Fast multi-class dictionaries learning with geometrical directions

in MRI reconstruction," IEEE Transactions on Biomedical Engineering, 2015.
R. Timofte, V. De, and L. V. Gool, "Anchored neighborhood regression for fast example-based super-resolution," in Proceed-ings of the 14th IEEE International Conference on Computer Vision (ICCV '13), pp. 1920–1927, Sydney, Australia, December 2013.
W. Wu, X. Yang, Y. Pang, J. Peng, and G. Jeon, "A multifocus image fusion method by using hidden Markov model," Optics Communications, vol. 287, pp. 63–72, 2013.
M. Perd'och, O. Chum, and J. Matas, "Efficient representation of local geometry for large scale object retrieval," in Proceedings of the IEEE Conference on Computer Vision and Pattern Recogni-tion (CVPR '09), pp. 9–16, Miami, Fla, USA, June 2009.
A. K. Jain, N. K. Ratha, and S. Lakshmanan, "Object detection using gabor filters," Pattern Recognition, vol. 30, no. 2, pp. 295–309, 1997.